



# MnCO<sub>3</sub>-Catalyzed Transesterification of Alcohols with Dimethyl Carbonate Under Mild Conditions

Xiuru Bi<sup>1,2</sup> · Nan Yao<sup>1</sup> · Xu Meng<sup>1</sup> · Mingxia Gou<sup>1</sup> · Peiqing Zhao<sup>1</sup>

Received: 6 May 2020 / Accepted: 5 July 2020  
© Springer Science+Business Media, LLC, part of Springer Nature 2020

## Abstract

Dimethyl carbonate (DMC) is a valuable green reagent with versatile and tunable chemical reactivity and can be used as a raw material for transesterification of alcohols. Herein, MnCO<sub>3</sub> was found to be an efficient heterogeneous catalyst for transesterification of various alcohols with DMC and gave desired products under mild conditions. The MnCO<sub>3</sub> catalysts were fully characterized by XRD, BET, SEM, TEM, FT-IR and NH<sub>3</sub>-TPD. The analysis results indicated that MnCO<sub>3</sub> calcined at 300 °C has significantly enhanced surface area and abundant weak acid sites, which contributed to the superior catalytic performance in the transesterification. Furthermore, deactivation of catalyst resulted from the change of crystal structure and the decrease of weak acid sites. This research expands the potential application for DMC in green chemistry.

---

**Electronic supplementary material** The online version of this article (<https://doi.org/10.1007/s10562-020-03310-z>) contains supplementary material, which is available to authorized users.

---

✉ Xu Meng  
xumeng@licp.cas.cn

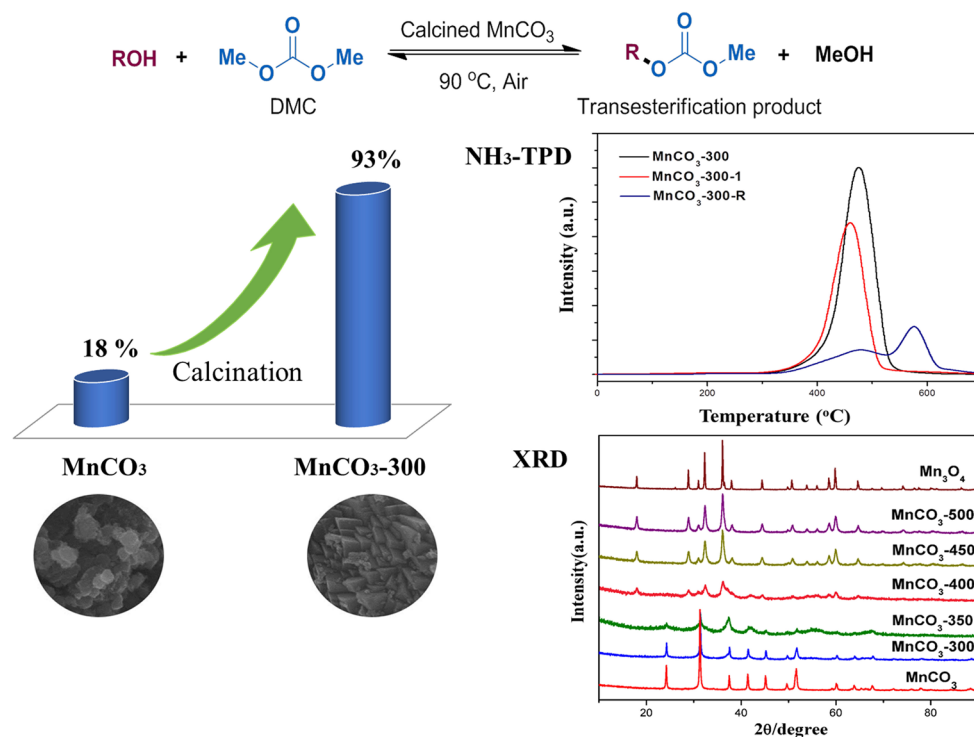
✉ Peiqing Zhao  
zhaopq@licp.cas.cn

<sup>1</sup> State Key Laboratory for Oxo Synthesis and Selective Oxidation, Suzhou Research Institute of LICP, Lanzhou Institute of Chemical Physics (LICP), Chinese Academy of Sciences, Lanzhou 730000, China

<sup>2</sup> University of Chinese Academy of Sciences, Beijing 100049, China

## Graphic Abstract

In this work,  $\text{MnCO}_3$  was found to be an efficient heterogeneous catalyst for transesterification of various alcohols with DMC and gave desired products under mild conditions.



**Keywords** Dimethyl carbonate ·  $\text{MnCO}_3$  · Transesterification · Heterogeneous catalysis · Selective catalysis

## 1 Introduction

Catalytic transesterification is one of the most desirable reactions for the synthesis of various esters in terms of atom economy, practicality, substrate generality, and functional group tolerance [1–5]. Dimethyl carbonate (DMC) as a valuable green reagent with versatile and tunable chemical reactivities was frequently used as a transesterification agent [6–16]. In addition, it is non-toxic, biodegradable, relatively inert, safe and widely used as a green solvent in organic synthesis [17]. However, most of transesterification reactions employing DMC as the raw material are homogeneous processes which show some disadvantages, such as difficulties in separation and purification of products, and recycling of the catalyst [18, 19]. Therefore, from an environmentally friendly point of view, the development of heterogeneous catalytic system in green medium for the transesterification is of great significance. Previously, heterogeneous catalysts have been developed, such as NaX [20], NaY [21],  $\text{K}_2\text{CO}_3$  [22],  $\text{Al}_2\text{O}_3$  [23] and  $\text{TiO}_2$  [24]. In the past years, our group has focused on the preparation and modification

of Mn-based materials and utilization of them as heterogeneous catalysts with redox and Lewis acid properties in many organic transformations [25–28]. Very recently, we found that  $\text{MnCO}_3$  calcined at the certain temperature could proceed transesterification rather than expected oxidation from the reaction of benzyl alcohol and DMC. Herein, as a part of our continuing efforts on developing sustainable catalytic systems [29–35], calcined  $\text{MnCO}_3$  was proved to be an efficient catalyst for transesterification of alcohols with dimethyl carbonate. The catalytic system over calcined  $\text{MnCO}_3$  could tolerate various alcohols as raw materials to react with DMC and led to desired products under mild conditions without any aldehydes from oxidation of alcohols. Scheme 1 shows the general transesterification reaction used in this study.

## 2 Experimental Section

All reagents were purchased from commercial suppliers and used without further purification and DMC (CAS NO. 616-38-6, ReagentPlus®, 99%) was purchased from

Sigma-Aldrich with a mark of Greener Alternative Product. All experiments were carried out under air. Flash chromatography was carried out with Merck silica gel 60 (200–300 mesh). Analytical TLC was performed with Merck silica gel 60 F254 plates, and the products were visualized by UV detection. The reaction was monitored and analyzed through a gas chromatograph (Agilent 7890A) with a flame ionization detector (FID). <sup>1</sup>H NMR and <sup>13</sup>C NMR (400 and 100 MHz, respectively) spectra were recorded in CDCl<sub>3</sub>. Chemical shifts (δ) are reported in ppm using TMS as the internal standard, and spin–spin coupling constants (J) are given in Hz.

## 2.1 Catalyst Preparation and Recycling

MnCO<sub>3</sub> calcined at 300 °C, 350 °C, 400 °C, 450 °C and 500 °C under air for 3 h in a muffle furnace was named as MnCO<sub>3</sub>-300, MnCO<sub>3</sub>-350, MnCO<sub>3</sub>-400, MnCO<sub>3</sub>-450 and MnCO<sub>3</sub>-500, respectively. When the MnCO<sub>3</sub>-catalyzed transesterification was finished, the catalyst was separated by centrifugation and washed by EtOH. After that, the extracted catalyst was dried in an oven at 60 °C for overnight. The used MnCO<sub>3</sub>-300 was recycled according to the above method. The MnCO<sub>3</sub>-300 used once, twice, three times were labeled as MnCO<sub>3</sub>-300-1, MnCO<sub>3</sub>-300-2, MnCO<sub>3</sub>-300-3, respectively. In order to recover the catalyst activity, we calcined MnCO<sub>3</sub>-300-1 at 300 °C for 3 h in air and it was labeled as MnCO<sub>3</sub>-300-R.

## 2.2 Catalyst Characterization Methods

The crystal structure and composition of catalysts were determined by powder X-ray diffraction using an X-Pert PRO X-ray diffractometer with CuKα radiation in the 2θ range of 10–90°. Infrared spectra of the catalyst samples were recorded with calcined powders embedded in KBr (2 mg of the sample in 300 mg of KBr) using a Perkin-Elmer One FT-IR spectrometer with a resolution of 4 cm<sup>-1</sup> operating in the range 500–2000 cm<sup>-1</sup> with 4 scans per spectrum. The morphology of the samples was characterized by using a TF20 transmission electron microscope and SM-5600LV scanning electron microscope. Nitrogen adsorption–desorption measurements were performed at 76 K using an ASAP 2020 M analyzer utilizing the BET model for the calculation of specific surface areas. The acid properties of the catalysts

were measured by the NH<sub>3</sub> temperature programmed desorption (NH<sub>3</sub>-TPD) technique. 50 mg of MnCO<sub>3</sub> samples was placed in a quartz reactor that was connected to a TPD apparatus, and the reactor was heated from room temperature to 800 °C with a heating rate of 10 °C min<sup>-1</sup>. The reducing atmosphere was a mixture of NH<sub>3</sub> and N<sub>2</sub> with a total flow rate of 30 mL min<sup>-1</sup> and the amount of NH<sub>3</sub> uptake during the reduction was measured by using a thermal conductivity detector (TCD).

## 2.3 Transesterification of Alcohols and DMC

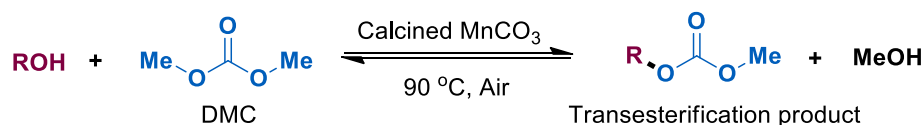
0.2 mmol of alcohol and 20 mg of MnCO<sub>3</sub> catalyst (8.5 mol%) were incorporated into a reactor containing 1.0 mL of DMC. The reaction mixture was heated at 90 °C for 8 h under vigorously stirring in air. The reaction was monitored by thin-layer chromatography (TLC). After completing the reaction, pure product was obtained by silica gel chromatography with petroleum ether/ethyl acetate (10: 1, v/v) as the mobile phase. The conversion and the selectivity of the reaction were obtained on the basis of GC analysis (dodecane was used as the internal standard reference).

## 3 Results and Discussion

### 3.1 Characterization of MnCO<sub>3</sub> Catalysts

Firstly, MnCO<sub>3</sub> and calcined ones were characterized by XRD, SEM, TEM, BET, FT-IR and NH<sub>3</sub>-TPD. In Fig. 1, the characteristic diffraction peaks of MnCO<sub>3</sub> were maintained in MnCO<sub>3</sub>-300 and MnCO<sub>3</sub>-350 (JCPDS file #44-1472). However, the diffraction peaks of them became broader, which indicates that the crystallite size of calcined materials gradually decreased. Notably, the XRD diffraction pattern of MnCO<sub>3</sub>-400 changed significantly, which means calcination at 400 °C could decompose MnCO<sub>3</sub> and led to formation of Mn<sub>3</sub>O<sub>4</sub> phase (JCPDS file #24-743). When the calcination temperature rose to 450 and 500 °C, the characteristic diffraction peak of Mn<sub>3</sub>O<sub>4</sub> in the samples became sharper and stronger, as a result of grain growth. Subsequently, the BET surface areas and porosities of the MnCO<sub>3</sub> materials were determined by N<sub>2</sub> adsorption–desorption (Table 1). It is obvious that the calcination treatment could significantly affect the BET surface area of MnCO<sub>3</sub>, the

**Scheme 1** MnCO<sub>3</sub>-catalyzed DMC transesterification reaction with ROH



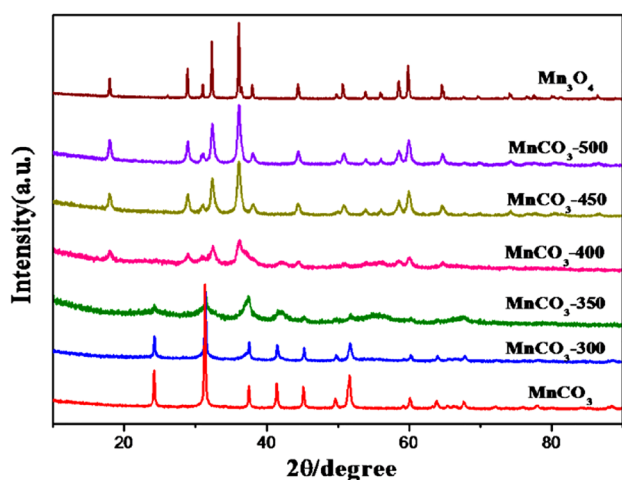


Fig. 1 XRD patterns of  $\text{MnCO}_3$  and calcined ones

Table 1 Textural properties of  $\text{MnCO}_3$  samples

Entry	Catalyst	Surface area ( $\text{m}^2\text{g}^{-1}$ )	Pore volume ( $\text{cm}^3\text{g}^{-1}$ )	Pore size (nm)
1	$\text{MnCO}_3$ -300	59.83	0.13	8.83
2	$\text{MnCO}_3$ -350	122.27	0.24	7.91
3	$\text{MnCO}_3$ -400	110.39	0.28	10.48
4	$\text{MnCO}_3$ -450	57.28	0.24	17.11
5	$\text{MnCO}_3$ -500	39.84	0.27	27.62
6	$\text{MnCO}_3$ -300-1	53.71	0.14	11.04
7	$\text{MnCO}_3$ -300-R	110.40	0.22	8.96
8	$\text{MnCO}_3$	10.78	0.04	14.48

surface area increased from 10.78 to 59.83  $\text{m}^2/\text{g}$  for  $\text{MnCO}_3$  and  $\text{MnCO}_3$ -300, respectively. However, as the temperature increased, the specific surface area of  $\text{MnCO}_3$ -400,  $\text{MnCO}_3$ -450 and  $\text{MnCO}_3$ -500 decreased gradually. Considering the results of XRD, it is concluded that the BET surface area decreased when crystal phase of calcined  $\text{MnCO}_3$

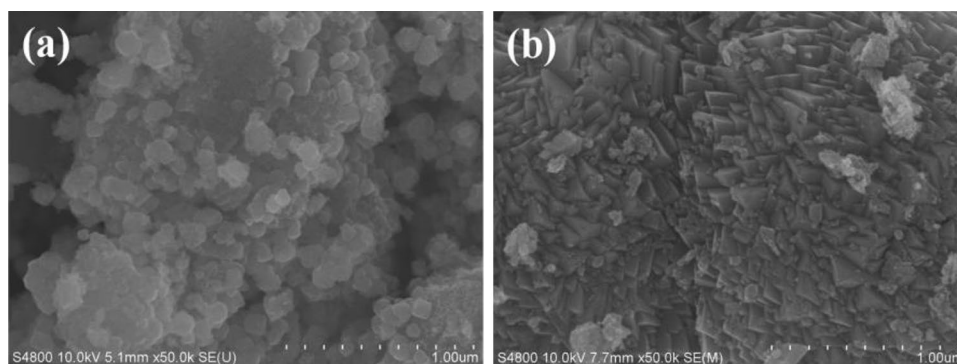
transferred to  $\text{Mn}_3\text{O}_4$ . From the SEM images (Fig. 2), it can be seen that the commercially purchased  $\text{MnCO}_3$  has a granular micro morphology. However, the  $\text{MnCO}_3$ -300 particles showed a cubic edge structure, which indicates that calcination treatment changed the morphology of the  $\text{MnCO}_3$ .

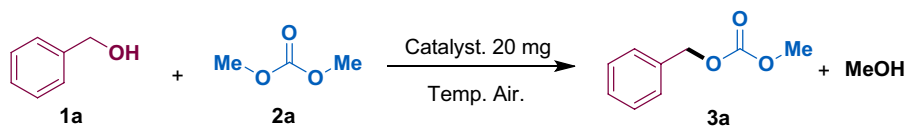
### 3.2 Catalytic Properties of $\text{MnCO}_3$ Catalysts

In an initial experiment, benzyl alcohol **1a** was used as model substrate with DMC in catalytic reaction system. In order to obtain highest yield, we screened the calcination temperature of  $\text{MnCO}_3$  catalysts. Firstly, blank experiment indicated that the reaction did not occur in the absence of catalyst in DMC at 90 °C (Table 2, entry 1). When commercial  $\text{MnCO}_3$  was used as the catalyst, unsatisfactory conversion was obtained. Although the conversion is about 18%, **3a** was the sole product and the selectivity was close to 100% (Table 2, entry 2). Then, we applied the  $\text{MnCO}_3$  catalysts after calcination at different temperatures to the reaction system, and  $\text{MnCO}_3$ -300 showed the best catalytic performance (Table 2, entries 3–7). Among the examined catalysts, the best result of 93% conversion and 100% selectivity were given by  $\text{MnCO}_3$ -300 catalyst.  $\text{MnCO}_3$ -350 with low crystallinity and others with  $\text{Mn}_3\text{O}_4$  crystal phase all showed poor activity. It was worthy to note that the reaction temperature affected the reaction obviously and the reaction temperature of 90 °C could give a high yield of 93% (Table 2, entry 3). When the temperature dropped below 90 °C, the etherification product **3a** was not detected at all and benzaldehyde was observed more or less.

Next, various alcohols were employed in the reaction to examine the reaction scope. In order to improve conversion of different substrates substituents, the reaction time was extended to 15 h. The results indicate that the  $\text{MnCO}_3$ -300 catalyst could catalyze various benzyl alcohols to react with DMC smoothly (Table 3). The conversions of the reaction were not obviously affected by electronic effect of the substrates and heterocyclic alcohols proceeded the reactions successfully. Unfortunately, phenyl propanol only gave a

Fig. 2 SEM images of a  $\text{MnCO}_3$ ; b  $\text{MnCO}_3$ -300



**Table 2** Optimization of reaction conditions

Entry	Catalyst	Temp.(°C)	Con.[%] <sup>a</sup>	Sel.[%] <sup>b</sup>
1	–	90	N.R	–
2	MnCO <sub>3</sub>	90	18	~ 99
3	MnCO <sub>3</sub> -300	90	93	~ 100
4	MnCO <sub>3</sub> -350	90	74	~ 99
5	MnCO <sub>3</sub> -400	90	67	~ 99
6	MnCO <sub>3</sub> -450	90	85	~ 100
7	MnCO <sub>3</sub> -500	90	72	~ 99
8	MnCO <sub>3</sub> -300-1	90	79	~ 99
9	MnCO <sub>3</sub> -300-2	90	67	~ 99
10	MnCO <sub>3</sub> -300-3	90	13	~ 99
11 <sup>c</sup>	MnCO <sub>3</sub> -300-R	90	89	0

Reaction conditions: benzyl alcohol (0.2 mmol), solvent DMC (1 mL), catalyst (20 mg), 90 °C, air (1 atm), 8 h

<sup>a</sup>The conversion and selectivity were obtained by GC using dodecane as an internal standard

<sup>b</sup>The product is benzaldehyde

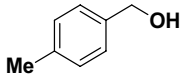
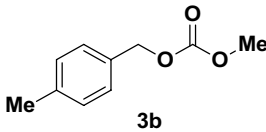
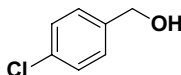
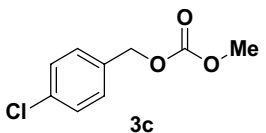
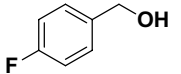
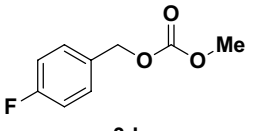
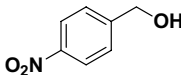
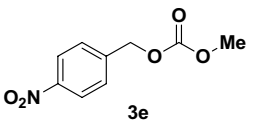
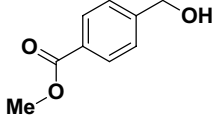
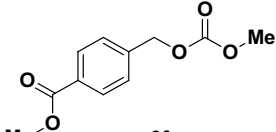
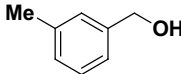
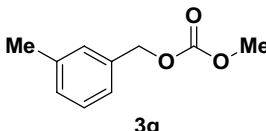
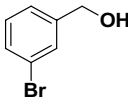
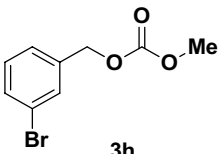
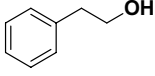
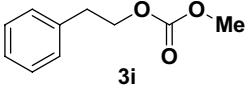
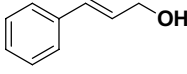
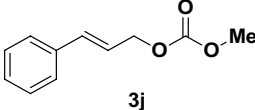
14% yield of desired product in the reaction because aliphatic substrate generally shows low activity.

### 3.3 The Stability and Deactivation of MnCO<sub>3</sub> Catalysts

Subsequently, the stability of MnCO<sub>3</sub>-300 was studied. Firstly, under the optimal reaction conditions, we examined the reusability of MnCO<sub>3</sub>-300. Unfortunately, with the reuse times increase, the catalytic performance decreased obviously (Table 2, entries 8–10). Next, we tried to recover the used catalyst by calcination of it at 300 °C for 3 h in air to restore its catalytic performance. By monitoring the reaction process, the results showed that the conversion of substrate **1a** was 89% using MnCO<sub>3</sub>-300-R as the catalyst. However, the obtained product is benzaldehyde from the oxidation of benzyl alcohol rather than **3a** by transesterification at all (Table 2, entry 11). After that, XRD, FT-IR, NH<sub>3</sub>-TPD, SEM/TEM and BET were used to study physicochemical properties of retrieved and recovered catalysts. The XRD patterns of the catalysts were not changed by repeated using of the catalyst (Fig. 3). However, calcination treatment of the retrieved MnCO<sub>3</sub>-300 changed the crystal structure greatly, and the crystalline phase was converted to ε-MnO<sub>2</sub> (JCPDS file #30-0820). Many studies have reported that MnO<sub>2</sub> materials have excellent oxidation properties [36–41], therefore benzyl alcohol was oxidized to benzaldehyde over

MnCO<sub>3</sub>-300-R. The XRD results are consistent with the catalytic experimental results (Table 2, entries 8–11). The lattice vibrational behavior of the MnCO<sub>3</sub> samples were studied by FT-IR spectroscopy to detect the effects of reusing and calcination treatment on the spectral features. From Fig. 4, we can see that MnCO<sub>3</sub>-300 and MnCO<sub>3</sub>-300-1 have similar IR spectra in the range of 1600–500 cm<sup>-1</sup>; both exhibit strong absorption bands located at 1440 cm<sup>-1</sup>, 860 cm<sup>-1</sup> and 730 cm<sup>-1</sup>, which are the characteristic absorption bands of MnCO<sub>3</sub>. [42–44] Here, the strong adsorption band at 1440 cm<sup>-1</sup> is attributed to the asymmetric stretching vibration of CO<sub>3</sub><sup>2-</sup> and another two strong and sharp adsorption bands at 730 cm<sup>-1</sup> and 860 cm<sup>-1</sup> can be regarded to be the out-of-plane bending and in-plane bending modes, respectively [45]. However, the characteristic absorption peaks of CO<sub>3</sub><sup>2-</sup> were disappeared in the MnCO<sub>3</sub>-300-R IR spectra, which means the MnCO<sub>3</sub> structure was changed after calcination treatment. Next, NH<sub>3</sub>-TPD was employed to investigate the L-acid properties of those catalysts (Fig. 5). The NH<sub>3</sub>-TPD patterns of MnCO<sub>3</sub>-300 and MnCO<sub>3</sub>-300-1 showed one weak acid sites absorption peak at 350–520 °C, while in addition to that, the MnCO<sub>3</sub>-300-R also has a strong acid sites adsorption peak at 520–620 °C. More importantly, the weak acid sites ratio was MnCO<sub>3</sub>-300 (0.68) > MnCO<sub>3</sub>-300-1 (0.39) > MnCO<sub>3</sub>-300-R (0.02), which is agreement with their catalytic activities in the transesterification (Table 2, entries 8–11). The sharp decrease of weak

**Table 3** The scope of the transesterification of alcohols and DMC

Entry	Substrate	Product	Yield (%) <sup>a</sup>	Conv. (%) <sup>b</sup>	Sel. (%)
	$  \begin{array}{c}  \text{R-OH} + \text{Me-O-C(=O)-O-Me} \xrightarrow[\text{Air, 15h}]{\text{MnCO}_3\text{-300, 20 mg}} \text{R-O-C(=O)-O-Me} + \text{CH}_3\text{OH} \\  \mathbf{1} \qquad \qquad \mathbf{2} \qquad \qquad \qquad \qquad \qquad \qquad \qquad \mathbf{3}  \end{array}  $				
1			96	96	100
2			66	66	100
3			55	55	100
4			61	61	100
5			72	72	100
6			69	69	100
7			54	54	100
8			14	14	100
9			91	91	100



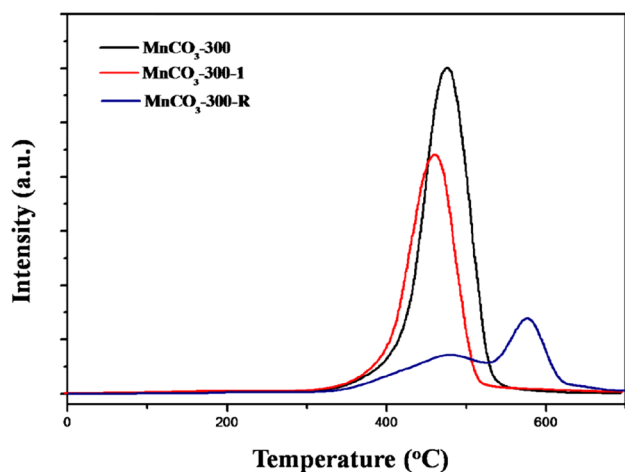


**Fig. 5**  $\text{NH}_3$ -TPD profiles of fresh  $\text{MnCO}_3$ -300,  $\text{MnCO}_3$ -300-1 and  $\text{MnCO}_3$ -300-R

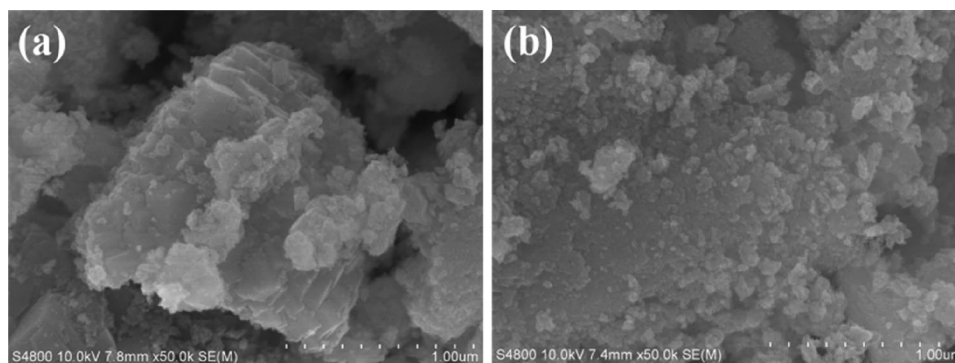
acid sites might lead to the activity loss of  $\text{MnCO}_3$ -300-R. Therefore, the enhanced surface area and abundant amounts of weak acid sites of  $\text{MnCO}_3$ -300 were believed to contribute to the superior catalytic activity. Also, it is speculated that the sharp decrease of weak acid sites and the change of crystal phase of retrieved ( $\text{MnCO}_3$ -300-1) and recovered ( $\text{MnCO}_3$ -300-R) catalysts lead to the loss of catalytic activity. Additionally, SEM images showed that  $\text{MnCO}_3$ -300-1 and  $\text{MnCO}_3$ -300-R both have granular morphology (Fig. 6).

Observed carefully, there is cubic structure in the surface of  $\text{MnCO}_3$ -300-1, which means the morphology of  $\text{MnCO}_3$ -300 does not change significantly after use. While the cubic edge structure disappeared in the  $\text{MnCO}_3$ -300-R indicating that the morphology of the catalyst changed with the phase transformation from  $\text{MnCO}_3$  to  $\epsilon$ - $\text{MnO}_2$  during the calcination process (for the TEM images, see SI, Fig. S1). Finally, it was found that the texture properties of  $\text{MnCO}_3$ -300-1 was remained and  $\text{MnCO}_3$ -300-R was changed remarkably due to the phase transformation (Table 1). The above observation from characterization of catalysts provides the reason why the catalyst lost catalytic activity gradually.

## 4 Conclusions

In conclusion, an efficient catalytic transesterification between alcohols and DMC over calcined  $\text{MnCO}_3$  was developed. The catalytic system tolerated a wide range of substrates and offered desired esterification products in good yields and selectivity. The full characterization of calcined  $\text{MnCO}_3$  demonstrated that the high crystallinity, enhanced surface area and abundant of weak acid sites were key factors for the superior catalytic activity. The  $\text{MnCO}_3$ -based catalytic system provides a more eco-friendly and practical method for transesterification reaction. The other application of  $\text{MnCO}_3$ -based catalysts in organic synthesis is ongoing in our laboratory.

**Fig. 6** SEM images of **a**  $\text{MnCO}_3$ -300-1; **b**  $\text{MnCO}_3$ -300-R



**Acknowledgements** We gratefully acknowledge the National Natural Science Foundation of China (Grant Nos. 21403256, 21573261), the Youth Innovation Promotion Association CAS (2018456).

## References

- Otera J (1993) *Chem Rev* 4:1449–1470
- Otera J (2003) In *Esterification*. Wiley, Chichester
- Hydonckx HE, De Vos DE, Chavan SA, Jacobs PA (2004) *Top Catal* 27:83–96
- Grasa GA, Singh R, Nolan SP (2004) *Synthesis* 7:971
- Maegawa Y, Ohshima T, Hayashi Y, Agura K, Iwasaki T, Mashima K (2011) *ACS Catal* 1:1178–1182
- Ono Y (1997) *Catal Today* 35:15–25
- Tundo P (2001) *Pure Appl Chem* 73:1117–1121
- Memoli S, Selva M, Tundo P (2001) *Chemosphere* 43:115–121
- Delledonne D, Rivetti F, Romano U (2001) *Appl Catal A* 221:241–251
- Chankeshwara SV (2008) *Synlett* 4:624–625
- Selva M, Perosa A (2008) *Green Chem* 10:457–464
- Arico F, Tundo P (2010) *Russ Chem Rev* 79:479–490
- Lissel M, Schmidt S, Neuman B (1986) *Synthesis* 5:382–383
- M. Lissel (1987) *Liebigs Ann Chem* 1:77–79
- Lee Y, Shimizu I (1998) *Synlett* 10:1063–1064
- Tundo P, Rossi L, Loris A (2005) *J Org Chem* 70:2219–2224
- Glasnov T, Holbrey J, Kappe C, Seddon K, Yan T (2012) *Green Chem* 14:3071–3076
- Tundo P, Selva M (2002) *Acc Chem Res* 35:706–716
- Xu B, Madix RJ, Friend CM (2011) *J Am Chem Soc* 133:20378–20383
- Selva M, Militello E, Fabris M (2008) *Green Chem* 10:73–79
- Bonino F, Damin A, Bordiga S, Selva M, Tundo P, Zecchina A (2005) *Angew Chem Int Ed* 117:4852–4855
- Fan MM, Zhang PB (2007) *Energy Fuels* 21:633–635
- Bai R, Wang Y, Wang S, Mei F, Li T, Li G (2013) *Fuel Process Technol* 106:209–214
- Zhang X, Ke X, Zheng Z, Liu H, Zhu H (2014) *Appl Catal B Environ* 150–151:330–337
- Meng X, Zhang J, Chen G, Chen B, Zhao P (2015) *Catal Commun* 69:239–242
- Meng X, Wang Y, Chen B, Chen G, Jing Z, Zhao P (2017) *Org Process Res Dev* 21:2018–2024
- Shen J, Meng X (2019) *Catal Commun* 127:58–63
- Shen J, Meng X (2020) *Catal Commun* 138:105846
- Huang Y, Zheng K, Liu X, Meng X, Astruc D (2020) *Inorg Chem Front* 7:939–945
- Bi X, Meng X, Chen G, Chen B, Zhao P (2018) *Catal Commun* 116:27–31
- Meng X, Wang Y, Chen B, Jing Z, Chen G, Zhao P (2017) *J Org Chem* 82:6922–6931
- Meng X, Bi X, Yu C, Chen G, Chen B, Jing Z, Zhao P (2018) *Green Chem* 20:4638–4645
- Liu X, Huang Y, Meng X, Li J, Wang D, Chen Y, Tang D, Chen B (2019) *Synlett* 30:1026–1036
- Meng X, Bi X, Yu C, Chen G, Chen B, Jing Z, Zhao P (2018) *Org Process Res Dev* 22:1716–1722
- Bi X, Tang T, Meng X, Gou M, Liu X, Zhao P (2020) *Catal Sci Technol* 10:360–371
- Jiang X, Gary P, Patel M, Zheng J, Yin J (2020) *J Mater Chem B* 8:1191–1201
- Voinov M (1982) *Electrochim Acta* 27:833–835
- Gude JC, Rietveld LC, Halem D (2017) *Water Res* 111:41–51
- Liu L, Floreancig PE (2010) *Org Lett* 12(20):4686–4689
- Cui YJ, Wang AZ, Wu L, Zhang X, Liu X (2017) *Sens Actuat B Chem* 252:30–36
- Yan G, Zhang Y, Di W (2018) *Analyst* 143:2915–2922
- Duan X, Lian J, Ma J, Kim T, Zheng W (2010) *Cryst Growth Des* 10:4449–4455
- Zhou T, Jiang X, Zhong C, Tang X, Ren S, Zhao Y, Liu M, Lai X, Bi J, Gao D (2016) *J Lumin* 175:1–8
- Wang L, Sun Y, Zeng S, Cui C, Li H, Xu S, Wang H (2016) *Cryst Eng Comm* 18:8072–8079
- Mu Y, Wang L, Zhao Y, Liu M, Zhang W, Wu J, Lai X, Fan G, Bi J, Gao D (2017) *Electrochim Acta* 104:119–128

**Publisher's Note** Springer Nature remains neutral with regard to jurisdictional claims in published maps and institutional affiliations.